

# PARAMETER IDENTIFICATION PROBLEMS IN STRUCTURAL AND GEOTECHNICAL ENGINEERING

By F. E. Udwadia,<sup>1</sup> J. A. Garba,<sup>2</sup> and Afshin Ghodsi<sup>3</sup>

**ABSTRACT:** This paper investigates some problems related to the ill-posedness of parameter identification problems which are commonly met with in structural and geotechnical engineering. Viewing the identification problem within a suitable framework, two basic types of ill-posedness are introduced. The first is inherent to the system (the governing differential equations), while the second is related to the type of data that is acquired at a given location (e.g., velocity, acceleration, etc.) and the basic algorithms used in the identification process. Examples of each type of ill-posedness are analyzed. Particular attention is given to the recurrent problem of identification of a nonconstant coefficient of a linear differential equation. Such coefficients often model the spatial variation of material properties in media. A method of handling spatially varying parameters for geotechnical applications is proposed. A general stochastic model for the parameter variation is used and it is shown that the identification problem using the Bayesian approach then leads to stable estimates, circumventing the instability problems of the direct inverse approach. Sensitivity studies are included to indicate the robust nature of the estimator. Simultaneous estimation of the "scatter" in the material property variation, and the material property parameter values themselves is next undertaken and it is shown that the method yields good estimates though the estimator now becomes a nonlinear function of the measurement. Simultaneous estimation of the measurement noise characteristics is also shown to be possible.

## INTRODUCTION

The identification problem for a system  $S$  can be looked at in terms of a class of models  $M$  under consideration, a class of inputs  $I$ , an error criterion  $\epsilon$ , an identification algorithm (estimator)  $E$ , and a set of parameters  $P$ . It generally takes the following form: Given the system response (measured at one or more locations in the system)  $R$ , for the class of inputs  $I$ , identify the set of parameters  $P$ , belonging to the class of models  $M$ , such that a suitable error criterion,  $\epsilon$ , is minimized. The error norm is generally related to a suitable norm of the difference between the system performance and the model response. Over the years various estimators,  $E$ , have been developed which are used in conjunction with various error criteria,  $\epsilon$ , to arrive at the "best" set of parameters that cause the model,  $M$ , to mimic the system response. However, little attention so far has been placed on the possible ill-posed nature of the identification problem. To systematize our ideas, the writers introduce in section I two distinct types of ill-posedness, which both could lead to erroneous results from the identification process. We will refer to the first

<sup>1</sup>Prof., Dept. of Civ. Engrg., Univ. of Southern California, Los Angeles, Calif. 90089.

<sup>2</sup>Jet Propulsion Lab., Pasadena, Calif.

<sup>3</sup>Grad. Student, Univ. of Southern California, Los Angeles, Calif.

Note.—Discussion open until February 1, 1985. To extend the closing date one month, a written request must be filed with the ASCE Manager of Technical and Professional Publications. The manuscript for this paper was submitted for review and possible publication on September 28, 1983. This paper is part of the *Journal of Engineering Mechanics*, Vol. 110, No. 9, September, 1984. ©ASCE, ISSN 0733-9399/84/0009-1409/\$01.00. Paper No. 19116.

variety as "inherent" ill-posedness and the second as "algorithmic" ill-posedness. Two examples of each type of ill-posedness are presented. The examples provided are pertinent in that they represent actual techniques that have been used in the past for identification of structural and geotechnical systems. In that sense, they are somewhat generic. It is shown that some of these techniques, if not applied carefully, could lead to significant errors when parameter values are estimated from actual test data.

Of special importance is example 4, in which the nonconstant coefficient function of a linear differential equation is to be identified from response data obtained under static loading conditions. In this case, the equation is that for a bending beam and the coefficient represents the variation of the bending rigidity along its length. It is shown that a straightforward approach to identifying the coefficient will lead to erroneous results because of the algorithmic ill-posedness of the problem. As several structural and geotechnical systems are modeled through the use of differential equations, special attention is paid to this generic problem in the remainder of this paper, and a technique for identification of such spatially-varying coefficients in differential equations is developed. In many applications, these spatially-dependent coefficients represent the variation of material properties from point to point in a medium.

In section II, we present a useful stochastic model for considering the spatial variability of material properties. That model is of great value in the areas of soil and geotechnical engineering, in which the material properties may vary, to an extent, randomly throughout a medium. The model includes a "random walk" type of process, along with a bias term which represents a priori knowledge, and encompasses deterministic and stochastic material property variations. Within the preview of such a realistic model of material property variations, section III addresses a commonly encountered set of problems involving the identification of material properties that spatially vary, in systems modeled by differential equations. The algorithmic ill-posedness illustrated in example 4 for such systems is removed by casting the problem within the framework of fixed interval smoothing techniques. A MAP estimator that is linear in the measurements is directly obtained. Sensitivity studies are included to show the robustness of the technique. The method is extended in section IV to simultaneously identify the realization of the random variation of material properties as well as the extent of the measurement noise. The optimal estimator is now a nonlinear function of the measurements. A quick and simple algorithm for solving the nonlinear problem is provided, and it is shown that the technique gives excellent results. Lastly, identification of the particular realization of the random spatial variation of material properties is attempted, in addition to the identification of the governing parameters that model the parent stochastic process, which generate that particular realization. Again, a nonlinear estimator results, and the algorithm previously developed is used to obtain good identification results.

**Inherent Ill-Posedness.**—When the identification process, using the class of inputs,  $I$ , and response,  $R$ , yields a set of parameters,  $P$ , which are nonunique, in a noiseless measurement environment, the system identification problem is said to be inherently ill-posed. We observe that

this ill-posedness is not related to the exact nature of the error criterion,  $\epsilon$ , or the estimator,  $E$ , used in the identification process, but the class of models,  $M$ , the class of inputs,  $I$ , and responses,  $R$ . Of course,  $I$  and  $R$  include, in their definitions, the locations at which the dynamic data are gathered for spatially distributed systems. The only possible way, then, in which this ill-posedness can be avoided is through the choice of a different class of inputs,  $I$ , or responses  $R$ , or both. This generally implies changed locations at which the inputs or responses, or both, are measured for the system.

*Example 1.*—Consider a soil system modeled by a vertical linear discrete shear beam, with  $N (>1)$  degrees of freedom. If for an input time history,  $I$ , at the base of the beam, the response is determined at any location other than the lowest discrete mass, the identification problem related to the determination of the stiffness distribution throughout the structure can become ill-posed. Thus, no matter what criterion  $\epsilon$  is chosen, or with what accuracy measurements are made, the results from identification using that data would always be suspect. On the other hand, if two  $N$ -degrees-of-freedom linear shear beams, which may differ possibly only in their stiffness distribution, have the same response  $R_i(t)$  at their lowest mass level for base motions  $I_i(t)$ , for all possible response-input pairs, i.e.  $i = 1, 2, \dots$ , then stiffness distributions of the two systems are completely identical. In other words, there are no inherent ill-posedness (base input—lowest mass response) pairs, as far as identifying the stiffness distribution of the system is concerned (7).

Fig. 1 exemplifies that type of situation. Consider a physical system modeled by the two degree-of-freedom model shown on the left in Fig. 1(a). If the response of mass  $m_1$ , caused by a base motion  $z(t)$ , is measured, then such data would not be able to unequivocally determine which of the two models shown in Fig. 1 represents the actual physical system. Both the systems shown [with  $m_R = m_1/(m_1 + m_2)$ ] would yield identical

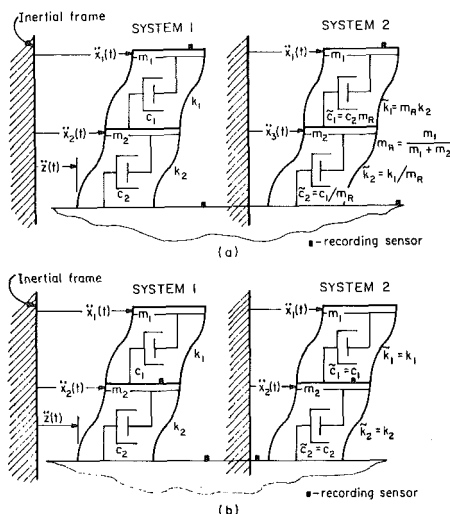


FIG. 1.—Two Degree-of-Freedom Model

responses at mass  $m_1$  to whatever base motion is applied. On the other hand, if the two systems shown in Fig. 1(b) have identical responses of mass  $m_2$  for each and every base input  $z(t)$ , we can be sure that both the systems must have identical properties.

Fig. 2 shows the response of the systems shown in Fig. 1(a) to a base acceleration. We note that the response of the mass  $m_1$  is identical in both cases. Fig. 3 shows the error in the base shear as a function of the base excitation frequency when the "incorrect" model is picked due to this inherent nonuniqueness. It is, therefore, errors in parameters, such as the base shear, that cause the problems of ill-posedness to be significant from a practical engineering viewpoint.

*Example 2.*—In the modeling of systems that respond primarily in the linear range, it is often assumed that if the model frequencies coincide with the measured frequencies of vibration of the actual system, the cor-

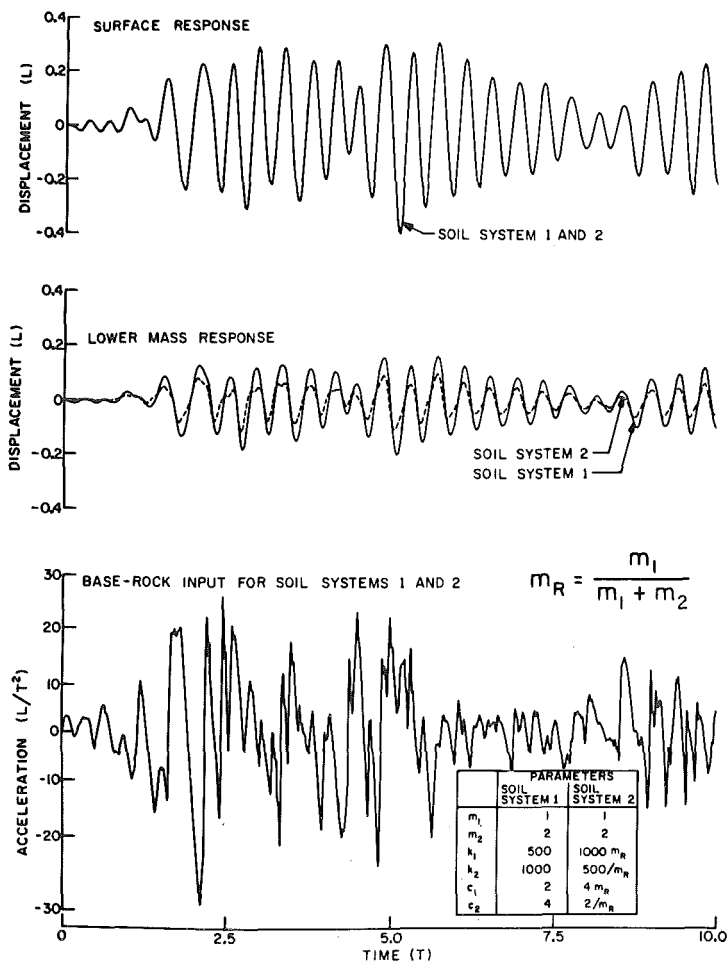


FIG. 2.—Response to Base Acceleration

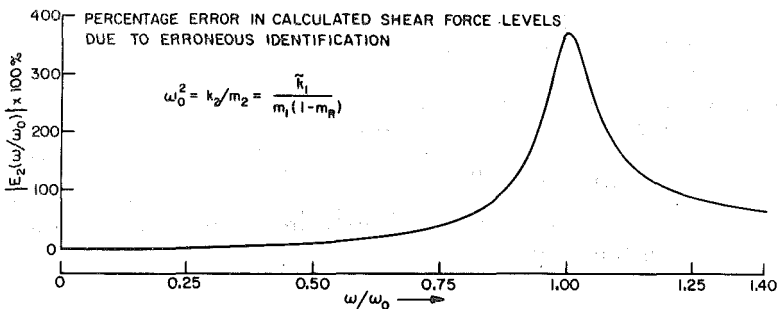


FIG. 3.—Error in Base Shear as Function of Base Excitation Frequency

rect parameter identification of the system has been accomplished. That this assumption is incorrect and would, therefore, lead to erroneous parameter values can be illustrated through a simple example (8).

Consider a structure modeled by the system shown in Fig. 1(a). For expository purposes, let us assume that  $m_1 = m_2 = 1$  and that  $c_1 = c_2 = 0$ . The equation that governs the vibrational frequencies of the system can then be easily shown:

$$\lambda^2 - (2k_1 + k_2) + k_1k_2 = 0 \dots\dots\dots (1)$$

The roots of this equation are controlled by the coefficients  $(2k_1 + k_2)$  and  $k_1k_2$ . If we have two different models, as shown in Fig. 1, such that

$$2k_1 + k_2 = 2\tilde{k}_1 + \tilde{k}_2 \dots\dots\dots (2a)$$

$$\text{and } k_1k_2 = \tilde{k}_1\tilde{k}_2 \dots\dots\dots (2b)$$

then both systems will exhibit identical frequencies of vibration and yet have very different parameter values.

One can, however, uniquely identify the stiffness matrix in this example if, in addition, all the eigenvectors are measured, since the stiffness matrix,  $\mathbf{K}$ , can then be expressed as  $\mathbf{K} = \mathbf{P}^T\mathbf{\Lambda}\mathbf{P}$  when  $\mathbf{P}$  is the matrix of eigenvectors and  $\mathbf{\Lambda}$  is the diagonal matrix (in general, it is block Jordan) of eigenvalues. For large multi-degree-of-freedom systems, however, obtaining all the eigenvectors through measurements is difficult if not impossible.

The foregoing results, while perhaps having a mathematical flavor, are of great practical importance, since erroneous results will, in general, be obtained when inherent ill-posedness is present. Such a condition, as shown above, may lead to completely inaccurate estimates of quantities of engineering importance, such as the base shears and bending moments in systems modeled as shear or bending beams. It is noteworthy that the principal means of getting around this inherent identification problem is to move to a different geometric location in the structure or obtain more and different kinds of data, or both.

**Algorithmic Ill-Posedness.**—When the identification process yields a set of parameters  $\mathbf{P}$  which are unstable in the presence of measurement noise, the identification problem is algorithmically ill-posed. This sort of

ill-posedness can be generally remedied by a proper choice of the algorithms and by the type of data (i.e., displacement, velocity, etc.) that is collected.

*Example 3.*—Consider the identification of the mass  $m$  of a single-degree-of-freedom oscillator represented by the equation:

$$m\ddot{x} + c\dot{x} + kx = f(t); \quad x(0) = 0; \quad \dot{x}(0) = 0 \dots\dots\dots (3)$$

A simple algorithm for identifying  $m$  from the measurement of the response  $x(t)$  appears to be

$$m = \frac{\int_0^\epsilon f(t)dt}{\dot{x}(\epsilon)} \dots\dots\dots (4)$$

in which  $\epsilon =$  a very short interval of time. The approach seems straightforward enough and has been proposed by some researchers (5) for the identification of the inertial properties of a system. (We note that an extension to multi-degree-of-freedom systems is obvious.) However, if the measurement of  $x(t)$  is corrupted with noise so that

$$z(t) = x(t) + w(t); \quad |w(t)| \leq r|x(t)| \dots\dots\dots (5)$$

with  $r \ll 1$ , then the use of this noise corrupted data directly in the algorithm will yield

$$m^* = \frac{\int_0^\epsilon f(t)dt}{\dot{x}(\epsilon) + \dot{w}(\epsilon)} \dots\dots\dots (6)$$

Thus 
$$\frac{1}{m^*} - \frac{1}{m} = \frac{\dot{w}(\epsilon)}{\int_0^\epsilon f(t)dt} \dots\dots\dots (7)$$

Heuristically speaking, the error in estimating  $m$  is proportional to the derivative of the noise, which can be arbitrarily large even when the noise,  $w(x)$ , itself is very small. The identification of  $m$  using the preceding algorithm is an ill-posed problem. Small changes in the measurement will yield large changes in the values of the identified parameters. A more rigorous proof of the preceding statement may be found in Appendix I.

*Example 4.*—Consider a beam of spatially-varying stiffness governed by the relation

$$\frac{d^2}{dx^2} \left( EI(x) \frac{d^2u}{dx^2} \right) = q(x); \quad 0 \leq x \leq 1 \dots\dots\dots (8)$$

in which  $u =$  the deflection of the beam;  $q(x) =$  the uniformly distributed load on the beam. Identification of the coefficient  $EI(x)$  can be obtained by integrating Eq. 8 twice to yield

$$R(x) = [EI(x)]^{-1} = \frac{d^2u}{dx^2} \left[ \int_c^x \left\{ \int_a^b q(s) ds \right\} db + V(a)(x - c) + M(c) \right]^{-1} \frac{d^2u}{dx^2} F(x) \dots \dots \dots (9)$$

in which  $V(x)$  and  $M(x)$  denote the shear force and the bending moment at location  $x$ . Thus, if the load  $q(x)$  is known for all  $x$ ,  $0 \leq x \leq 1$ , and if at any two isolated locations on the beam, the shear force and bending moment are respectively known, the deflected shape of the beam then defines  $EI(x)$  uniquely through Eq. 9. The major problem here would be in determining the curvature of the beam accurately. For, if instead of  $u(x)$ , the quantity  $w(x)$  is measured, in which

$$w(x) = u(x) + z(x) \dots \dots \dots (10)$$

with  $z(x)$  being the measurement noise, the use of  $w(x)$  in Eq. 9 would lead to

$$R^*(x) = \frac{d^2w}{dx^2} F(x) \dots \dots \dots (11)$$

The estimation error then becomes

$$|R(x) - R^*(x)| = \left| \frac{d^2z}{dx^2} \right| |F(x)| \dots \dots \dots (12)$$

As noted earlier, even if  $|z(x)| \leq r|u(x)|$ , with  $r \ll 1$ , for all  $x$ , the derivatives of the measurement noise can be arbitrarily large, thereby causing estimation errors to be large, even when the noise  $z(x)$  itself is very small.

The interval  $[0,1]$  is discretized, and using a finite difference scheme, the displacement is determined at  $N = 46$  equispaced locations,  $(x_r; r = 0, 1, 2, \dots, 45)$ , along where  $x_0 = 0$  and  $x_{45} = 1$ . Fig. 4 shows  $a(x) \frac{d^2u}{dx^2} EI(x)^{-1}$ ,  $0 \leq x \leq 1$ , for a cantilever beam subjected to a constant distributed load of  $q(x) = (0.001) * (N)^2$  and an end moment of  $M_n = -0.03 * N^2$  (with the shear force known to be zero at  $x = 1$ ). The noise corrupted measurements are shown together with the "exact response" of the beam at these locations. The noise characteristics chosen are  $E[z_r] = 0$ , for  $r \in [0,45]$  and  $E[z_m, z_l] = \sigma_z^2 \delta_k(m - l)$  in which  $\delta_k$  is the Kroneker delta. Using this noisy data, with  $\sigma_z^2 = 1$ , an attempt is made to estimate  $a(x)$ , using Eq. 9. The estimation result indicated in Fig. 5 shows the algorithmic instability obtained when such an approach is used. Despite the relatively low level of the measurement noise (see Fig. 4), the values of  $a(x)$  are incorrect and oscillate between  $\pm 300$ . Comparing the true values of  $a(x)$  with those obtained (Fig. 5), we find that the errors are roughly in excess of about an order of magnitude.

The obvious prescription for such a situation is to 'filter' out the measurement noise and 'smooth' out the displacement data. However, the extent to which the data may be smoothed out is a matter of some importance, since it will affect not only the estimate of the coefficient function  $EI(x)$ , but also our level of confidence in that estimate.

The identification of spatially-varying coefficients that are embedded

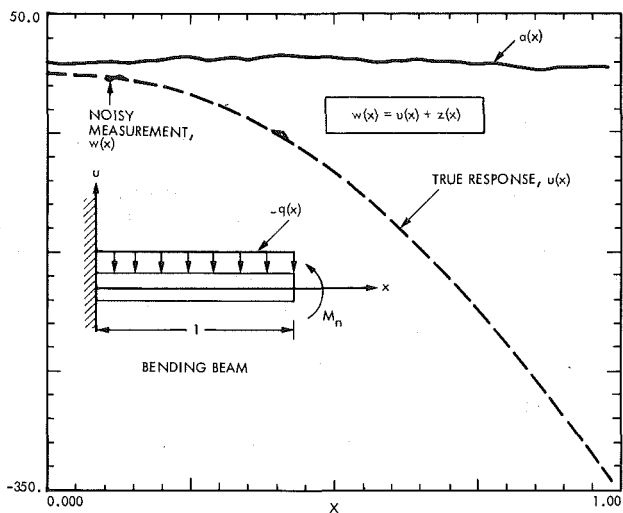


FIG. 4.—Cantilever Beam Subjected to Constant Distributed Load and End Moment

in differential equations could lead to highly erroneous results, if not done with care. As problems of this generic nature are recurrent in the modeling of structural and geotechnical systems, the remainder of this paper concentrates on building the techniques for the identification of

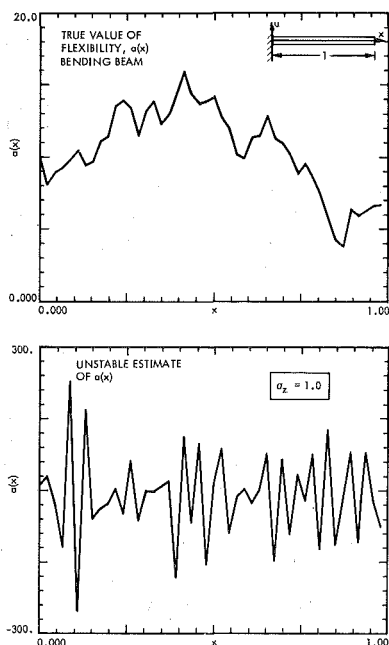


FIG. 5.—Estimation Result



those coefficients. These spatially-varying coefficients often represent the varying material properties of the medium under consideration. First, let us then consider a realistic model for representing the variation of material properties in a medium, and then set about developing stable identification procedures.

**Different Approach to Spatial Variability.**—Consider for simplicity, a material property,  $a$ , that depends on one space dimension,  $x$ . Let us discretize (digital computations normally demand discretization) the  $x$ -domain at locations  $x_i$ ,  $i \in [0, N]$ , in which  $N$  can be any large number. Then, a model of spatial variability that appears to be useful especially in geotechnical application is

$$a(x_{i+1}) = \alpha_{i+1}a(x_i) + \epsilon_{i+1} + \eta_{i+1} \dots \dots \dots (13)$$

in which  $a(x_i)$  denotes the material properties at location ' $i$ ';  $\{\alpha_i\}$ ,  $\{\eta_i\}$  are assumed to be known a priori sequences; and  $\{\epsilon_i\}$  is a sequence of random numbers, which, in general, are correlated with each other. That model embodies the following physical situations: (1) If  $\alpha_i = 0 = \epsilon_i$ ,  $\forall i$ , the material properties are deterministically known since  $\{\eta_i\}$  is assumed to be known a priori; (2) if  $\alpha_i = 0$ , the variability in material properties is given by

$$a(x_{i+1}) = \epsilon_{i+1} + \eta_{i+1}, \quad \forall i \dots \dots \dots (14)$$

Thus,  $a(x_i)$  is represented to have a value that 'deviates' from a 'nominal value' by a random amount  $\epsilon_i$ . The random variable  $\epsilon_i$  then, obviously, represents the uncertainty in our knowledge of the material property at location  $i$ ; and (3) if  $\eta_i = 0$ ,  $\forall i$ , then the variability in material properties can be expressed as

$$a(x_{i+1}) = \alpha_{i+1}a(x_i) + \epsilon_{i+1} \dots \dots \dots (15)$$

The value of  $r$  at location ' $i + 1$ ' is deterministically dependent on its value at location ' $i$ ' and deviates from it by a random variable  $\epsilon_i$ . If, the random variables  $\epsilon_i$  are independent, then  $a(x_i)$  becomes a Markov process. A better understanding of Eq. 15 can be obtained if we further put  $\alpha_i = 1$ ,  $\forall i$ . Then the model represents a 'random-walk' process, often called a drunkard's walk, in which the value of the property at location  $i + 1$  constitutes a random step of size  $\epsilon_{i+1}$  from its value at step  $i$ . There is considerable evidence to indicate that such random-walk models are applicable to many materials, especially earth media (1,2,4). If, further  $\eta_i \neq 0$ ,  $\forall i$ , we have a sort of a "biased" random-walk (much like that of a drunkard attempting to move towards a liquor bar!).

**Some Applications of Spatial Variability Model.**—In this section, we consider two applications of the preceding model. The first deals with the identification of the flexibility along the length of a bending beam given the moment  $M$  at one location and the shear force  $V$  at another, from measurements taken along the length of the beam. The second deals with the identification of the shearing rigidity of a shear beam given measurements along it and the shear force at one location on it. In each case, we note that we are dealing, in general, with the identification of the realization of a random process.

For simplicity of exposition, the steady state situation (static) is considered. Using a finite difference approach it is shown, in each case, that

the problem can be rephrased as a linear dynamic system amenable to the techniques of fixed interval smoothing. A Bayesian estimation scheme is developed and the identification carried out.

A numerical example is included to indicate the strengths of the method proposed, and the ability with which the scheme can identify not just the distributed parameters, but also quantities like the measurement noise variance and the variance of the random sequence  $\epsilon_i$ , should these two parameters be constant and not known a priori, with great accuracy.

*Example 5.*—Consider a segment of unit length of a bending beam governed by the differential equation

$$\frac{d^2}{dx^2} \left( \frac{1}{a(x)} \frac{d^2 u}{dx^2} \right) = q(x), \quad 0 \leq x \leq 1 \dots\dots\dots (16)$$

in which  $q(x)$  = the distributed load on the beam; and  $a(x)$  = its flexibility. Let us say that at two locations on the beam the following data are available:

$$V(x = 1) = V_0; \quad M(x = 0) = M_0 \dots\dots\dots (17)$$

Identification of  $a(x)$  from noisy measurements of  $u$  (the deflection of the beam) at various locations  $x$  for this steady-state problem will be analyzed.

A direct integration of Eq. 16 can be easily shown to yield

$$a(x) = \left( \frac{d^2 u}{dx^2} \right) \left[ M_0 + V_0 x - \int_0^x \left[ \int_y^1 q(z) dz \right] dy \right]^{-1} \dots\dots\dots (18)$$

The determination of  $a(x)$  from such a relationship using measurements  $w(x)$  which are corrupted by noise  $z(x)$ , in which

$$w(x) = u(x) + z(x) \dots\dots\dots (19)$$

will lead to an ill-posed problem causing the estimates of  $a(x)$  to be unstable, as shown before. Let us begin by discretizing the space variable and considering a finite difference form for Eq. 16. We assume that the measurement noise is Gaussian in nature. Let  $x = i\Delta x$ ,  $i = 0, 1, \dots, N$ . Then Eqs. 16–18 can be expressed as

$$\frac{D_{i-1}}{a_{i-1}} - 2 \frac{D_i}{a_i} + \frac{D_{i+1}}{a_{i+1}} = q_i (\Delta x)^2 = \bar{q}_i, \quad i = 1, 2, \dots, N - 1 \dots\dots\dots (20a)$$

$$\frac{D_N}{a_N} - \frac{D_{N-1}}{a_{N-1}} = V_0 \Delta x = \bar{V}_0 \dots\dots\dots (20b)$$

$$\frac{D_0}{a_0} = M_0 \dots\dots\dots (20c)$$

$$w_i = u_i + z_i, \quad i = -1, 0, 1, \dots, N \dots\dots\dots (20d)$$

when  $D_i = (d^2 u / dx^2)_i$  and the subscript  $i$  denotes the quantity evaluated at  $x = x_i$ . We note that  $w$  is measured at  $x = -\Delta x$  also. Eqs. 20a–20d can be recast by telescoping them to yield

$$\frac{D_{i+1}}{a_{i+1}} = \frac{D_i}{a_i} - (\bar{\gamma}_i - \bar{V}_0), \quad i = 0, 1, 2, \dots, N - 2; \quad \frac{D_0}{a_0} = M_0 \dots\dots\dots (21a)$$

with  $\tilde{\gamma}_i = \sum_{r=i+1}^{N-1} \tilde{q}_r \dots \dots \dots (21b)$

Using again a central difference scheme as before, the displacements can now be expressed by the recursive relations

$$u_{i+1} = 2u_i - u_{i-1} + a_i(M_0 - R_i)(\Delta x)^2, \quad i = 0, 1, \dots, N - 1 \dots \dots \dots (22a)$$

in which  $R_i = \sum_{l=0}^{i-1} (\tilde{\gamma}_l - \tilde{V}_0)$ , with  $R_0 \Delta 0 \dots \dots \dots (22b)$

When the spatial variation of  $a(x)$  is modeled by

$$a_{i+1} = \alpha_{i+1} a_i + \epsilon_{i+1} + \eta_{i+1}, \quad i = 0, 1, 2, \dots, N - 2 \dots \dots \dots (23)$$

then the system of equations formed by Eqs. 22-23 and the observation equation, Eq. 20d, represents a third-order discrete linear dynamic system with state  $(\underline{y}_i, a_i)$  (in which  $\underline{y}_i = [u_i, u_{i-1}]^T$ ), and the determination of the system state becomes a fixed interval smoothing problem. We note that the system response is, in general, dependent through the recursive Eq. 22 on  $u_0$  and  $u_{-1}$ , which are not known a priori and need to be estimated. Also, Eq. 23 prescribes  $a_{i+1}$  in terms of  $a_i$ , but  $a_0$  is not known a priori, and, therefore, also needs to be estimated. Defining,

$$[\epsilon_1, \epsilon_2, \dots, \epsilon_{N-1}]^T = \underline{\epsilon}; \quad [a_0, a_1, \dots, a_{N-1}, u_0, u_{-1}]^T = \underline{\theta};$$

$$[w_{-1}, w_0, w_1, \dots, w_N] = \underline{W}; \quad [u_{-1}, u_0, u_1, \dots, u_N] = \underline{U};$$

$$[z_{-1}, z_0, z_1, \dots, z_N] = \underline{Z}; \quad \text{with } E[Z^T Z] = \Sigma, \quad E[e^T e] = H \dots \dots \dots (24)$$

we can now express Eq. 23 as

$$\underline{\epsilon} = A \underline{\theta} - \underline{\eta} \dots \dots \dots (25)$$

in which  $A = \begin{bmatrix} -\alpha_1 & 1 & & & & 0 & 0 & 0 \\ & -\alpha_2 & 1 & & & 0 & 0 & 0 \\ & & \cdot & \cdot & & \cdot & \cdot & \cdot \\ & & & \cdot & \cdot & \cdot & \cdot & \cdot \\ & & & & \cdot & \cdot & \cdot & \cdot \\ & & & & & 0 & 0 & 0 \\ & & & & & -\alpha_{N-1} & 1 & 0 & 0 \end{bmatrix} \dots \dots \dots (26)$

and  $\underline{W} = \underline{U} + \underline{Z} = B \underline{\theta} + \underline{Z} \dots \dots \dots (27)$

$$B = \begin{bmatrix} 0 & 0 & \cdot & \cdot & \cdot & \cdot & \cdot & 0 & 1 \\ 0 & 0 & \cdot & \cdot & \cdot & \cdot & \cdot & 1 & 0 \\ M_0(\Delta x)^2 & 0 & \cdot & \cdot & \cdot & \cdot & \cdot & 2 & -1 \\ 2M_0(\Delta x)^2 & (M_0 - R_1)(\Delta x)^2 & \cdot & \cdot & \cdot & \cdot & \cdot & 3 & -2 \\ 3M_0(\Delta x)^2 & 2(M_0 - R_1)(\Delta x)^2 & (M_0 - R_1)(\Delta x)^2 & \cdot & \cdot & \cdot & \cdot & 4 & -3 \\ 4M_0(\Delta x)^2 & 3(M_0 - R_1)(\Delta x)^2 & 2(M_0 - R_2)(\Delta x)^2 & (M_0 - R_3)(\Delta x)^2 & \cdot & \cdot & \cdot & 5 & -4 \\ 5M_0(\Delta x)^2 & 4(M_0 - R_1)(\Delta x)^2 & 3(M_0 - R_2)(\Delta x)^2 & 2(M_0 - R_3)(\Delta x)^2 & \cdot & \cdot & \cdot & \cdot & \cdot \\ \cdot & \cdot & \cdot & \cdot & \cdot & \cdot & \cdot & \cdot & \cdot \\ \cdot & \cdot & \cdot & \cdot & \cdot & \cdot & \cdot & \cdot & \cdot \\ NM_0(\Delta x)^2 & (N-1)(M_0 - R_1)(\Delta x)^2 & \cdot & \cdot & \cdot & \cdot & \cdot & N+1 & -N \end{bmatrix} \dots \dots \dots (28)$$

Downloaded from ascelibrary.org by SOUTHERN CALIFORNIA UNIVERSITY on 02/15/14. Copyright ASCE. For personal use only; all rights reserved.

The MAP estimate  $\theta$  can be found by maximizing the density  $p_{\theta|W}(\underline{a}, \underline{d}) \triangleq p_{W|\theta}(\underline{d}|\underline{a}) p_{\theta}(\underline{a})$ .

The expression for  $p_{W|\theta}(\underline{d}|\underline{a})$  is

$$(2\pi)^{\frac{-N+1}{2}} |\Sigma|^{-1/2} \exp \left[ -\frac{1}{2} (\underline{d} - B\underline{a}) \Sigma^{-1} (\underline{d} - B\underline{a}) \right] \dots \dots \dots (29)$$

in which  $|\Sigma|$  is the determinant of  $\Sigma$ , and the expression for  $p_{\theta}(\underline{a})$  can be expressed as

$$p_{\theta}[a_1, a_2, \dots, a_{N-1}|a_0, u_0, u_{-1}] p(a_0, u_0, u_{-1}) \dots \dots \dots (30)$$

As  $a_0, u_0, u_{-1}$  are all unknown a priori, their density may be omitted from the maximization process. Furthermore

$$\epsilon_i = a_i - \alpha_i a_{i-1} - \eta_i, \quad i = 1, 2, \dots, N \dots \dots \dots (31)$$

so that  $p_{\theta}[a_1, a_2, \dots, a_{N-1}|a_0, u_0, u_{-1}] = p_e[A\underline{\theta} - \underline{\eta}] \left| \frac{\partial \epsilon_i}{\partial a_j} \right| \dots \dots \dots (32)$

Noting that  $|\partial \epsilon_i / \partial a_j| = 1$ , the MAP estimator then requires the minimization of

$$J \triangleq (\underline{d} - B\underline{a})^T \Sigma^{-1} (\underline{d} - B\underline{a}) + (A\underline{a} - \underline{\eta})^T H^{-1} (A\underline{a} - \underline{\eta}) \dots \dots \dots (33)$$

with respect to  $\underline{a}$ . The estimate  $\hat{\underline{a}}$  thus reduces to

$$\hat{\underline{a}} = [B^T \Sigma^{-1} B + A^T H^{-1} A]^{-1} [A^T H^{-1} \underline{\eta} + B^T \Sigma^{-1} \underline{d}] \dots \dots \dots (34)$$

with the error covariance given by

$$E[(\underline{\theta} - \hat{\underline{\theta}})(\underline{\theta} - \hat{\underline{\theta}})^T] = (B^T \Sigma^{-1} B + A^T H^{-1} A)^{-1} \dots \dots \dots (35)$$

The MAP estimator is linear in the measurements  $\underline{d}$ , and is unbiased. Fig. 6 shows the application of Eqs. 34 and 35 for the situation described in section 2 (Fig. 4), in which the covariance matrices  $\mathbf{H}$  and  $\Sigma$  are defined by  $H_{ij} = \delta_k(i - j)\sigma_{\epsilon}^2$  and  $\Sigma_{ij} = \delta_k(i - j)\sigma_z^2$ . Thus, matrices  $\mathbf{H}$  and  $\Sigma$  will reduce to diagonal matrices, with  $\sigma_{\epsilon}^2$  and  $\sigma_z^2$  in their diagonals, respectively. In this example, the bias term sequence  $\{\eta_i\} = \{0\}$  and the set  $\{\alpha_i\} = 1.0$ . With these relations we can simplify Eqs. 34 and 35 to

$$\text{(Eq. 34a): } \hat{\underline{\theta}} = \left[ B^T B \frac{\sigma_{\epsilon}^2}{\sigma_z^2} + A^T A \right]^{-1} \left[ B^T \underline{d} \frac{\sigma_{\epsilon}^2}{\sigma_z^2} \right]$$

$$\text{(Eq. 35a): } E[(\underline{\theta} - \hat{\underline{\theta}})(\underline{\theta} - \hat{\underline{\theta}})^T] = \left[ B^T B \frac{\sigma_{\epsilon}^2}{\sigma_z^2} + A^T A \right]^{-1} \cdot \sigma_{\epsilon}^2$$

The figure shows the estimate when  $\sigma_z = 1$  and  $\sigma_{\epsilon} = 1$ , with  $1 - \sigma$  error bands. As  $\sigma_z^2$ , the variance in the measurement noise decreases to zero, the estimate of  $a(x)$  improves, and the  $1 - \sigma$  error band narrows in width. From Eq. 34a we can see that the estimate  $\hat{\underline{\theta}}$  is dependent only on the ratio of  $\sigma_{\epsilon}^2$ , while the error covariance matrix is dependent on the ratio stated earlier and also,  $\sigma_{\epsilon}^2$ . Fig. 7 shows the relation between root-mean-square error in the estimate of  $a(x)$ , which is given by

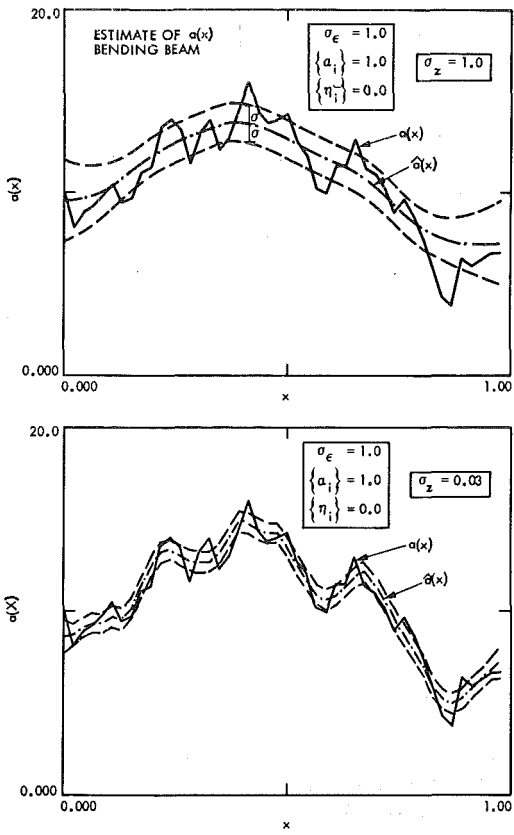


FIG. 6.—Application of Eqs. 34–35

$$E_a = \left[ \frac{1}{N} \sum_{i=0}^{N-1} \left( \frac{\hat{a}_i - a_i}{a_i} \right)^2 \right]^{1/2} \dots \dots \dots (36)$$

and different ratios of variances,  $\sigma_z^2/\sigma_\epsilon^2$ , produced by keeping  $\sigma_\epsilon^2 = 1.0$  and by changing the variance in the measurement noise,  $\sigma_z^2$ . Fig. 7 also shows the relation between the mean of the trace of the covariance matrix given by Eq. 35a and the same ratios of variances. As the variance in the measurement noise increases ( $\sigma_z^2/\sigma_\epsilon^2$  increases), both the root-mean-square error in the estimate of  $a(x)$  and mean of the trace of the covariance matrix increase. The rms error is relatively small ( $<0.5$ ), even when  $\sigma_z/\sigma_\epsilon \approx 7$ .

Example 6.—Consider a system modeled by the differential equation

$$\frac{d}{dx} \left( \frac{1}{a(x)} \frac{du}{dx} \right) = -q(x), \quad 0 \leq x \leq 1 \dots \dots \dots (37)$$

with  $\frac{1}{a(1)} \frac{du}{dx} \Big|_{x=1} = V \dots \dots \dots (38)$

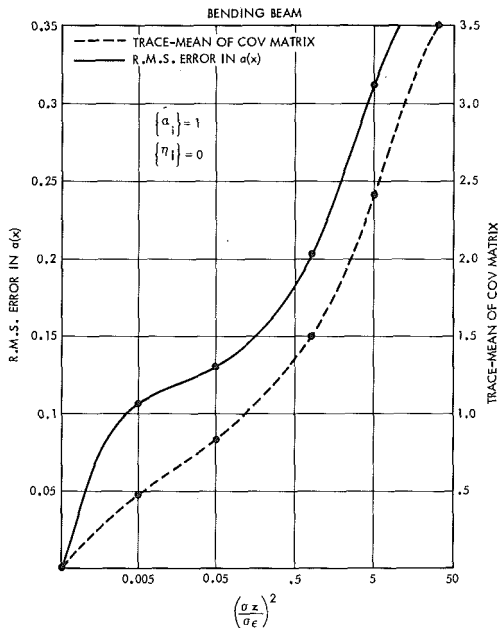


**FIG. 7.—Relation Between Root Mean Square Error in Estimate of  $a(x)$  and Different Ratios of Variances**

Those equations could be viewed as governing the deflections,  $u$ , of a shear beam whose flexibility,  $a$ , varies with the  $x$  direction and which is subjected to a shear force,  $V$ , at  $x = 1$ . Alternatively,  $u$  can be thought of as the hydraulic head in an inhomogeneous aquifer;  $q(x)$ , the flow rate of aquifer subcharge;  $a(x)^{-1}$  the aquifer transmissibility; and  $V$ , the normal flux at  $x = 1$ . Identification of  $a(x)$  from measurements of  $u(x)$  is sought. A direct integration of Eq. 37 can be easily shown to yield

$$a(x) = \left( \frac{du}{dx} \right) \left\{ V + \int_x^1 q(x) dx \right\}^{-1} \dots \dots \dots (39)$$

The determination of  $a(x)$  from that type of relationship using measurements  $w(x)$ , which are corrupted by zero mean Gaussian white noise,  $z(x)$ , will lead, as before, to unstable estimates of  $a(x)$ .

As in the case of the bending beam, the interval  $[0, 1]$  is discretized and the displacement is determined at  $N = 46$  equispaced locations along it. Fig. 8(a) shows  $a(x)$  for a cantilever beam subjected to a constant distributed load of  $q(x) = 0.001/N^2$  and an end shear  $V = 0.005/N^2$ . The noise-corrupted "measurements," with variance  $\sigma_z^2 = 1.0$ , are shown together with "true response" of the beam. Fig. 9(a) shows the unstable estimate of  $a(x)$  using Eq. 39. The values of  $a(x)$  are incorrect and oscillate between  $+0.70E + 04$  and  $-0.10E + 04$ .

Then Eqs. 37, 38, and 19 can be expressed as

$$\frac{1}{a_i} (u_{i+1} - u_i) - \frac{1}{a_{i-1}} (u_i - u_{i-1}) = q_i (\Delta x)^2 = \bar{q}_i, \quad i = 0, 1, \dots, N - 1 \dots \dots (40a)$$

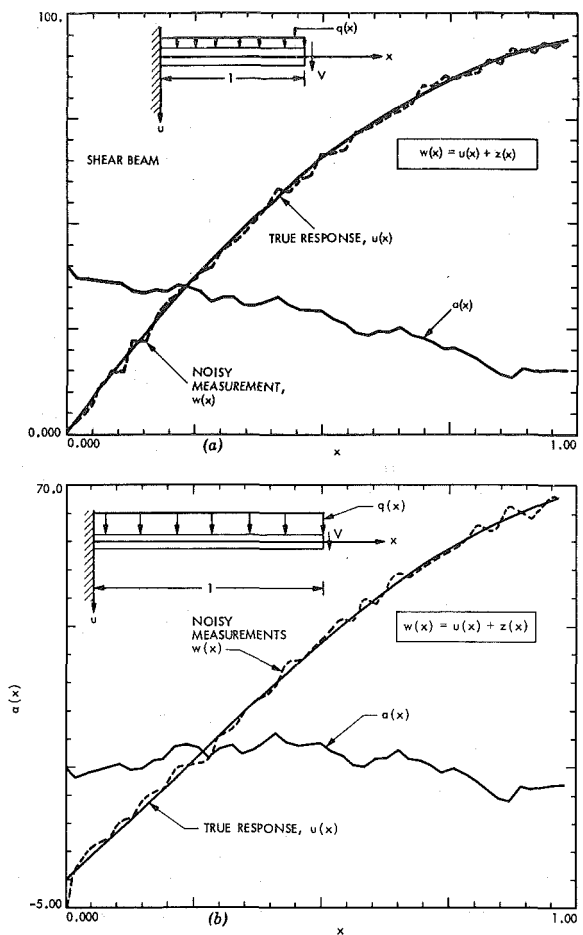


**FIG. 8.—(a)  $a(x)$  for Cantilever Beam Subjected to Constant Distributed Load and End Shear; (b) Identification Results for  $a(x)$  for Shear Beam when Bias Term Sequence is Set to Zero**

$$\frac{1}{a_N} (u_N - u_{N-1}) = V \Delta x = \bar{V} \dots (40b)$$

$$w_i = u_i + z_i, \quad i = 0, 1, \dots, N \dots (40c)$$

in which the subscript  $i$  indicates the quantity at location  $x_i = i \Delta x$ . Eqs. 40a-c can be recast by telescoping them to yield

$$u_{i+1} = u_i + a_i \{ \bar{V} - \bar{\gamma}_i \}, \quad i = 0, 1, \dots, N - 1 \dots (41a)$$

$$\text{in which } \bar{\gamma}_i = \sum_{l=i+1}^{N-1} \bar{q}_l \text{ and } \bar{\gamma}_N \triangleq 0 \dots (41b)$$

Also, the spatial variability of the medium can be represented by the relation

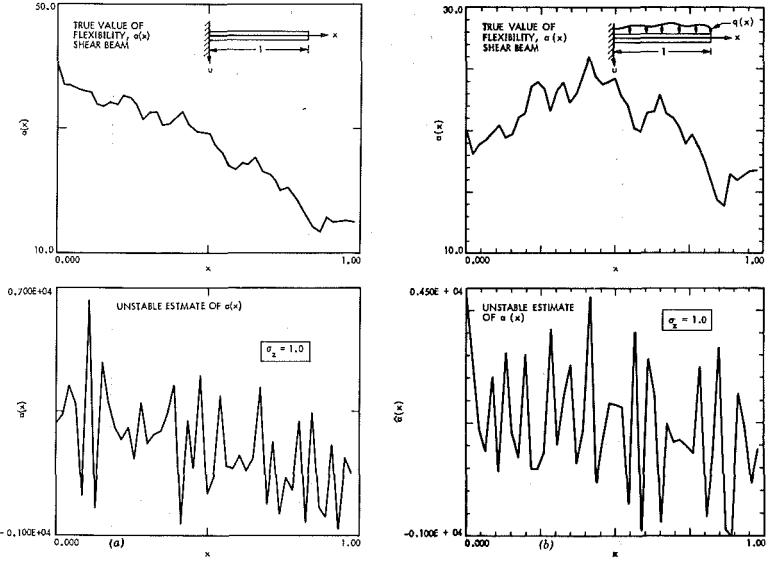


**FIG. 9.—(a) Unstable Estimate of  $a(x)$  Using Eq. 39; (b) Identification Results for  $a(x)$  for Shear Beam when Bias Term Sequence is Set to Zero**

$$a_{i+1} = \alpha_{i+1} a_i + \epsilon_{i+1} + \eta_{i+1} \dots \dots \dots (42)$$

in which  $\{\epsilon_i\}$  = a zero mean, Gaussian sequence and the  $\eta_i$  and  $\alpha_i$  are known a priori. Defining

$$\begin{aligned} [\epsilon_1, \epsilon_2, \dots, \epsilon_{N-1}]^T &\triangleq \underline{\epsilon}; & [a_0, a_1, \dots, a_{N-1}, u_0] &\triangleq \underline{\theta}; \\ [w_0, w_1, \dots, w_N]^T &\triangleq \underline{\omega}; & [u_0, u_1, \dots, u_N]^T &\triangleq \underline{u}; \dots \dots \dots (43) \end{aligned}$$

together with  $E\{zz^T\} = \Sigma$ ,  $E\{ee^T\} = H$  Eqs. 41–42 can be expressed by  $e = A\theta - \eta$  (Eq. 25a); and  $\psi = u + z = B\theta + z$  (Eq. 27a) with

$$A = \begin{bmatrix} -\alpha_1 & 1 & & & & & & 0 \\ & & \ddots & & & & & 0 \\ & & & \ddots & & & & 0 \\ & & & & \ddots & & & 0 \\ & & & & & \ddots & & 0 \\ & & & & & & \ddots & 0 \\ & & & & & & & -\alpha_{N-1} & 1 & 0 \end{bmatrix} \dots \dots \dots (44a)$$

$$\text{and } B = \begin{bmatrix} 0 & 0 & 0 & 1 \\ V + \tilde{\gamma}_0 & 0 & 0 & 1 \\ & V + \tilde{\gamma}_1 & 0 & 1 \\ & & 0 & 1 \\ & & & 0 \\ V + \tilde{\gamma}_0 & V + \tilde{\gamma}_1 & V + \tilde{\gamma}_{N-1} & 1 \end{bmatrix} \dots \dots \dots (44b)$$



The MAP estimator again leads to the Eqs. 34 and 35 for  $\hat{\theta}$ .

As stated before the covariance matrices  $\mathbf{H}$  and  $\Sigma$  are diagonal, defined by  $H_{ij} = \delta_k(i - j) \sigma_\epsilon^2$  and  $\Sigma_{ij} = \delta_k(i - j) \sigma_z^2$ . In this example,  $\{a_i\} = 1.0$ , and our priori knowledge of material properties is defined by the function  $a(x) = 10/(0.25 + 0.3x)$ . The bias term sequence, which is the difference between adjacent values of  $a(x)$ , is defined by

$$\frac{da(x)}{dx} = \{\eta_{i+1}\} = \frac{-3N}{(0.3i + 0.25N)^2} \dots \dots \dots (45a)$$

in which  $x = \frac{i}{N}$ ,  $i \in (0, N - 1) \dots \dots \dots (45b)$

With these relationships, Eqs. 34 and 35 will be simplified to

(Eq. 34a):  $\hat{\theta} = \left[ B^T B \frac{\sigma_\epsilon^2}{\sigma_z^2} + A^T A \right]^{-1} \left[ A^T \eta + B^T d \frac{\sigma_\epsilon^2}{\sigma_z^2} \right]$

(Eq. 35a):  $E[(\theta - \hat{\theta})(\theta - \hat{\theta})^T] = \left[ B^T B \frac{\sigma_\epsilon^2}{\sigma_z^2} + A^T A \right]^{-1} \cdot \sigma_\epsilon^2$

Fig. 10(a) shows the application of Eqs. 34 and 35 for the shear beam shown in Fig. 8(a), in which  $\sigma_z^2 = 1$  and  $\sigma_\epsilon^2 = 1$ . The estimate of  $a(x)$  is shown with  $1 - \sigma$  error bands. As before, as  $\sigma_z^2$  decreases to zero, the estimate of  $a(x)$  improves and the  $1 - \sigma$  error band narrows in width.

By setting  $\sigma_\epsilon^2 = 1.0$  and changing  $\sigma_z^2$ , the relationship between root mean square error in estimate of  $a(x)$  and the ratio of our variances,  $\sigma_z^2/\sigma_\epsilon^2$ , is computed [Fig. 11(a)]. Fig. 11(a) also shows the relationship

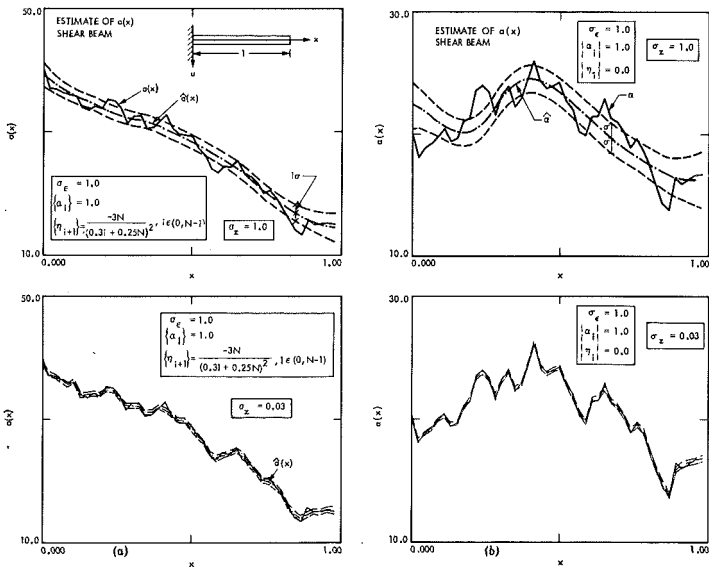
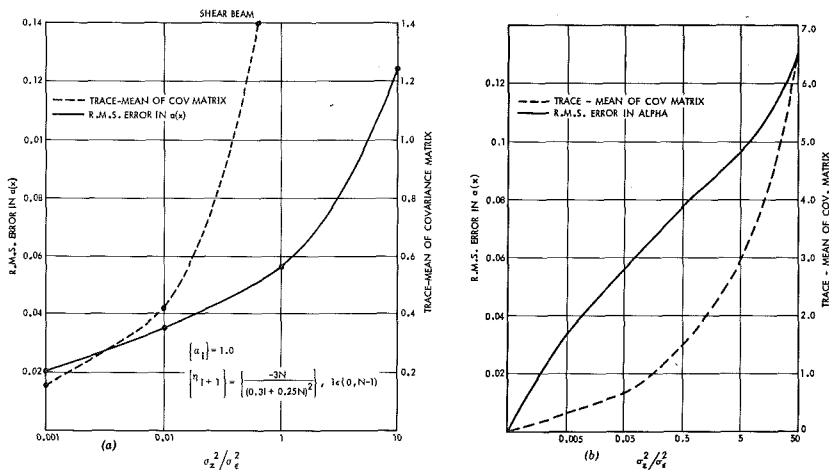


FIG. 10.—(a) Application of Eqs. 34–35 for Shear Beam of Fig. 8(a); (b) Identification Results for  $(a)x$  for Shear Beam when Bias Term Sequence is Set to Zero



**FIG. 11.—(a) Relationship Between Root Mean Square Error in Estimate of  $a(x)$  and Ratio of Variances; (b) Identification Results for  $a(x)$  for Shear Beam when Bias Term Sequence is Set to Zero**

between the mean of the trace of the covariance matrix given by Eq. 35a and the ratios of variances. As in the case of bending beam, rms error in estimate of  $a(x)$  and mean of the trace of covariance matrix both increase as the variance in the measurement noise increases.

When the bias term sequence  $\{\eta_{ij}\}$  is set to zero, the identification results for  $a(x)$  for the shear beam (when all else is the same as before) are shown in Figs. 8(b), 9(b), 10(b), and 11(b).

**Simultaneous Identification.**—In the numerical example shown in Fig. 8(b), we have assumed a knowledge of  $\Sigma$  and  $H$ . Often, only an estimate of the covariance matrix of the material property variation  $H$  may be available. In this section, the identification of  $\sigma_\epsilon$  is undertaken simultaneously with the realization of the random process  $a(x)$  when  $H_{ij} = \sigma_\epsilon^2 \delta_{ik} \delta_{kj}$  ( $i = j$ ). The variance at each step,  $\epsilon_i$  is considered constant and  $\{\epsilon_i\}$  is taken to be a zero mean, white noise sequence.

Taking the negative logarithm of  $p_{\theta,w}(a, d)$  and ignoring the constant terms, we define the function,  $L$ , for the situation exhibited by example 7 as

$$L(\theta, \sigma_\epsilon) = \ln p_{\theta,w}(a, d) = (N - 1) \ln \sigma_\epsilon + \left(\frac{1}{2}\right) J(a, \sigma_\epsilon) \dots \dots \dots (46)$$

in which  $J$  is defined by Eq. 33 and is also to be considered as a function of  $\sigma_\epsilon$ . Minimizing  $L(\theta, \sigma_\epsilon)$  with respect to  $\theta$  and  $\sigma_\epsilon$  then leads to

$$\hat{\sigma}_\epsilon = \frac{1}{N - 1} (A\hat{\theta})^T (A\hat{\theta}) \dots \dots \dots (47)$$

$$\hat{\theta} = \left[ B^T \Sigma^{-1} B + \frac{1}{\hat{\sigma}_\epsilon^2} A^T A \right]^{-1} \cdot [B^T \Sigma^{-1} d] \dots \dots \dots (48)$$

Eq. 47 represents a set of equations which yield the optimal estimates  $\hat{\theta}$  and  $\hat{\sigma}_\epsilon$ . The optimal estimator is now a nonlinear function of the measurement  $\hat{d}$  because  $\hat{\sigma}_\epsilon$  is itself a function of  $\hat{\theta}$ . Eqs. 47 and 48 can be solved in a three step procedure by: (1) Solving Eq. 48 for  $\hat{\theta}$ , using a sequence of values of  $\hat{\sigma}_\epsilon$ ; (2) for each  $\hat{\theta}$  so formed, using Eq. 47 to get an estimate of  $\sigma_\epsilon^*$ ; and (3) the optimal value of  $\hat{\sigma}_\epsilon$  is obtained by finding that value of  $\hat{\sigma}_\epsilon$  which satisfies  $\sigma_\epsilon^* = \hat{\sigma}_\epsilon$ .

The optimal estimate,  $\hat{\theta}$ , is now obtained from Eq. 48 by using this optimal value of  $\hat{\sigma}_\epsilon$ . This procedure is applied to the data shown in Figs. 8(b) and 9(b). Solution of the nonlinear set (Eqs. 47-48) is shown in Fig. 12. The optimal estimate of  $\hat{\sigma}_\epsilon$  is found to be 0.925, a value very close to the true value of  $\sigma_\epsilon = 1.0$ . The solution is clearly unique though the estimator is nonlinear. Thus, not only has the particular realization of the stochastic process  $a(x)$  been identified through this technique, but insight into the parameters that govern the parent stochastic process (which generates the realization is also obtained.

Similarly, it is often difficult to estimate the variance in the measurement noise (in particular if the "measurement chain" is fairly long). Assuming that  $\Sigma_{ij} = \sigma_z^2 \delta_k(i-j)$ , the variance of the measurement noise, given the values of  $\sigma_\epsilon$ , can be estimated through a similar minimization of the function

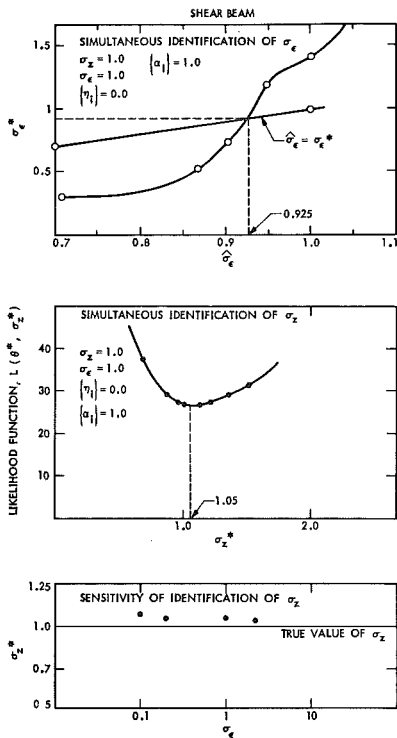


FIG. 12.—Solution of Nonlinear Set

$$L(\hat{\theta}^*, \sigma_z^*) = (N + 1) \ln \sigma_z^* + \left(\frac{1}{2}\right) J(a, \sigma_z^*) \dots \dots \dots (49)$$

in which  $J$  is again given by Eq. 33. Minimizing  $L(\hat{\theta}^*, \sigma_z^*)$  with respect to  $\hat{\theta}^*$  and  $\sigma_z^*$  gives

$$\hat{\sigma}_z^2 = \frac{1}{N + 1} (d - B\hat{a})^T (d - B\hat{a}) \dots \dots \dots (50)$$

$$\hat{\theta} = \left[ \frac{1}{\hat{\sigma}_z^2} B^T B + A^T H^{-1} A \right]^{-1} \left[ \frac{1}{\hat{\sigma}_z^2} B^T d \right] \dots \dots \dots (51)$$

The minimum value of  $L$  for various values of  $\sigma_z^*$  and corresponding values of  $\hat{\theta}^*$  (from Eq. 51) is obtained (Fig. 12). This value corresponds to the optimal estimate of  $\hat{\sigma}_z = 1.05$  which is very close to true value of  $\sigma_z = 1.0$ .

The sensitivity of our determination of  $\sigma_z$  to our knowledge or lack thereof of  $\sigma_\epsilon$  is shown in Fig. 12. There, the value of  $\sigma_z$  obtained for incorrectly assumed values of  $\sigma_\epsilon$  is shown. We observe that the estimator is very robust, providing good information on  $\sigma_z$  even in the absence of proper knowledge of  $\sigma_\epsilon$ . For the case when the bias term sequence  $\{\eta_{i+1}\} = -3N/(0.3i + 0.25N)^2, i \in (0, N-1)$ , Eqs. 47 and 48 will change to

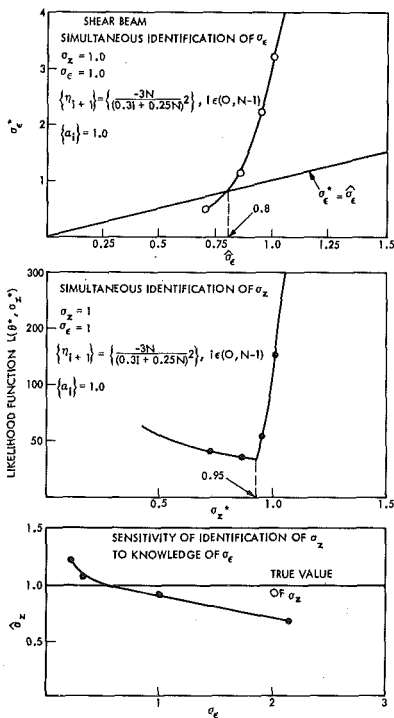
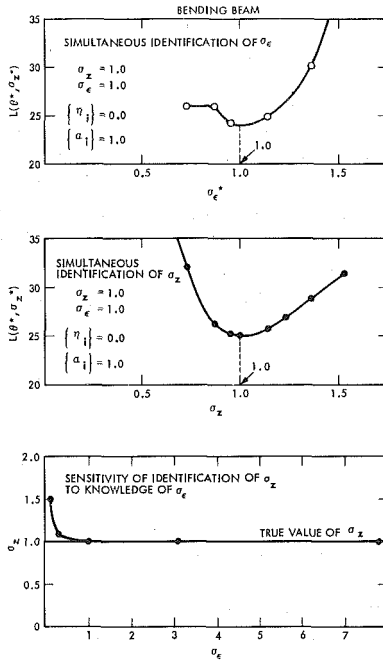


FIG. 13.—Optimal Estimate of  $\hat{\sigma}_z$



**FIG. 14.—Bending Beam Results**

$$\text{(Eq. 47a): } \hat{\sigma} = \frac{1}{N-1} (A\hat{\theta} - \eta)^T (A\hat{\theta} - \eta)$$

$$\text{(Eq. 48a): } \hat{\theta} = \left[ B^T \Sigma^{-1} B + \frac{1}{\hat{\sigma}_\epsilon^2} A^T A \right]^{-1} \cdot \left[ \frac{1}{\hat{\sigma}_\epsilon^2} A^T \eta + B^T \Sigma^{-1} d \right]$$

Using the data of Figs. 8(a) and 9(a), with the same procedure we can find the optimal estimate of  $\hat{\sigma}_\epsilon$ , found to be 0.8 (Fig. 13). Also, the variance  $\sigma_z$  can be estimated as before and yields a value of 0.95. The sensitivity of the estimate of  $\sigma_z$  to inaccurate knowledge of  $\sigma_\epsilon$  is also shown. Comparing with Fig. 12, the bias term  $\eta_i$  clearly increases this sensitivity of  $\sigma_z$ .

Similar results are received for the bending beam, as shown in Fig. 14. The data from Figs. 4 and 6 are used and the parameters  $\sigma_\epsilon$  and  $\sigma_z$  identified as before. The value of  $\hat{\sigma}_\epsilon$  is determined by plotting Eq. 46 for various values of  $\sigma_\epsilon^*$  and finding the minimum. Again, reasonably accurate estimates are obtained.

### CONCLUSIONS

This paper defines two concepts pertinent to parameter identification problems as applied in the fields of structural and geotechnical engineering. The ideas of inherent and algorithmic ill-posedness have been illustrated through examples taken from the current repertoire of system identification techniques. It is shown that several of these techniques,

some of which have been proposed as 'robust' in the past, are plagued by ill-posedness and will consequently yield erroneous parameter estimates. The concepts introduced here, we hope, will be useful in systematizing our thinking as regards the reliability of the results obtained by system identification methods, and will, hopefully, yield insights into improved methodologies for testing and analysis.

In the area of algorithmic ill-posedness, particular attention has been given to the identification of nonconstant coefficients that are embedded in linear differential equations. Such coefficients often represent spatial variations in material properties in media. The large number of systems that are modeled through such differential equations makes the proper identification of such coefficients an important issue. It is shown that straightforward approaches to this identification problem are algorithmically ill-posed.

Realizing that there is generally a stochastic component to the variation of material properties in most media (especially earth media), a stochastic model for the representation of such variations is proposed. The identification problem then reduces to the estimation of a spatially variable coefficient of a differential equation, the coefficient being the realization of a random process. For convenience the static, time independent problem is studied, and second- and fourth-order differential equations are considered. The stochastic variation leads to a fixed interval smoothing problem with the material property variation entering the state space of the dynamic linear model generated. A MAP estimation of the realization of the random process is obtained with the covariance matrix of the estimate.

The numerical examples chosen illustrate the robustness of the scheme and the ability of the technique to sense data that may sometimes be difficult to ascertain, such as the variability of the material properties,  $\sigma_\epsilon$ , or the level of the measurement noise,  $\sigma_z$ . Thus, not only does the method identify the realization of the random process that gives the spatial fluctuation of the material properties, but also the parameters that govern the parent stochastic process.

Such simultaneous identification, however, leads to the solution of a set of nonlinear equations, which are solved iteratively. Whereas we cannot guarantee the uniqueness of the solution of the nonlinear system, it appears that in the local vicinity of the correct parameters, minimization leads to a unique parameter set and accurate parameter estimates.

The stochastic model for material property variations in the medium proposed here, and the techniques developed for identifying the realization of such a stochastic variation, will be especially useful for the accurate assessment of small material property changes in fields, ranging from the construction and updating of nuclear facilities to the inflight assessment of material degradation for space vehicles. An imminent application area is that of early fault detection in large terrestrial and space structures.

## APPENDIX I.—PROOF

Consider the equation

$$m\dot{x} + kx = f(t); \quad \dot{x}(0) = x(0) = 0 \dots\dots\dots (52)$$

Denote the Fourier transforms by

$$X(w) = \frac{1}{2\pi} \int_{-\infty}^{\infty} x(t) e^{-iwt} dt \quad \text{and} \quad x(t) = \int_{-\infty}^{\infty} X(w)e^{iwt} dw \dots\dots\dots (53)$$

Eq. 52 can now be expressed as

$$m \int_{-\infty}^{\infty} -w^2 X(w) e^{iwt} dw + k \int_{-\infty}^{\infty} X(w)e^{iwt} dw = f(t) \dots\dots\dots (54)$$

Integration of Eq. 54 between  $-t_0$  and  $t_0$  gives

$$m \int_{-\infty}^{\infty} iwX(w)[e^{iwt_0} - e^{-iwt_0}] dw + k \int_{-\infty}^{\infty} \frac{X(w)}{iw} [e^{iwt_0} - e^{-iwt_0}] = g(t)$$

in which  $g(t) = \int_{-t_0}^{t_0} f(t)dt \dots\dots\dots (55)$

Given  $f(t)$ ,  $x(t)$ , and  $k$ , Eq. 55 can now be thought of as an algorithm for estimating  $m$ . Let us now consider a small variation  $\delta X(w)$ , caused possibly by measurement noise, and its consequent effect on the estimation of the parameter  $m$  through the use of Eq. 55. Denoting the variation in  $m$  by  $\delta m$ , we get

$$\begin{aligned} \delta m \int_{-\infty}^{\infty} iwX(w)[e^{iwt_0} - e^{-iwt_0}] dw &= -m \int_{-\infty}^{\infty} iw\delta X(w)[e^{iwt_0} - e^{-iwt_0}] dw \\ -k \int_{-\infty}^{\infty} \frac{\delta X(w)}{iw} [e^{iwt_0} - e^{-iwt_0}] dw &\dots\dots\dots (56) \end{aligned}$$

Furthermore, let the variation  $\delta X(w)$  have the form

$$\delta X(w) = \frac{1}{\sqrt{N}}, \quad N < |w| < N + 1, \quad N > 0 = 0, \quad \text{otherwise} \dots\dots\dots (57)$$

Eq. 53 then yields

$$\delta x(t) = \frac{2}{\sqrt{N}} \cos\left(N + \frac{1}{2}\right) t \frac{\sin t}{\frac{t}{2}} \dots\dots\dots (58)$$

so that the measurement noise  $\delta x(t) \rightarrow 0$  as  $N \rightarrow \infty$ . Using Eq. 57 in Eq. 56 then yields

$$\left| \frac{\delta m}{m} \right| \sim \frac{4}{\sqrt{N}} \int_N^{N+1} w \sin wt_0 dw - \frac{4k}{m\sqrt{N}} \int_N^{N+1} \frac{\sin wt_0}{w} dw \dots\dots\dots (59)$$

But  $\left| \int_N^{N+1} \frac{\sin wt_0}{w} dw \right| \leq \int_N^{N+1} \frac{1}{w} dw = \ln\left(1 + \frac{1}{N}\right) \dots\dots\dots (60)$

so that the second integral in Eq. 59 tends to zero as  $N \rightarrow \infty$ . The first integral in Eq. 59 can be simplified to yield

$$\frac{4}{\sqrt{N}} \left[ \frac{2}{t_0^2} \sin \frac{t_0}{2} \cos \left( N + \frac{1}{2} \right) t_0 - \frac{\cos (N + 1)t_0}{t_0} \right] + \frac{8\sqrt{N}}{t_0} \left[ \sin \frac{t_0}{2} \sin \left( N + \frac{1}{2} \right) t_0 \right] \dots \dots \dots (61)$$

Eq. 60 shows that  $|\delta m/m| \rightarrow \infty$  as  $N \rightarrow \infty$  i.e., as  $\delta x(t) \rightarrow 0$ , so that even vanishingly small amounts of measured noise could lead to arbitrarily large errors in the identification of  $m$  through Eq. 55. The addition of a damping term  $c\dot{x}$  on the right-hand side of Eq. 52, while increasing the algebraic complexity, will leave the result unchanged.

**APPENDIX II.—REFERENCES**

1. Anderson, B. D. O., and Moore, J. B., *Optimal Filtering*, Prentice-Hall, Inc., Englewood Cliffs, N.J., 1979.
2. Bastin, G., and Duque, C., "Modelling of Steady State Groundwater Flow Systems," *Proceedings of IASTED Symposium*, Switzerland.
3. Carotenuto, L., Raiconi, G., and DiPillo, G., "A Regularized Solution to the Identification Problem for the Distributed Parameter Model of an Underground Aquifer," *Proceedings IFAC Triennial World Congress*, Helsinki, Finland.
4. Delhomme, J. P., "Spatial Variability and Uncertainty in Groundwater Flow Parameters: A Geostatistical Approach," *Water Resources Research*, 15(2).
5. Masri, S. F., and Anderson, J. C., "Analytical and Experimental Studies of Nonlinear System Modellings," *NCR Report AT49-24-0262*, Apr., 1981.
6. Neuman, S. P., "Role of Subjective Value Judgement in Parameter Estimation," *Modelling and Simulation of Water Resources Systems*, Ed. Van Steenkiste, North Holland.
7. Udwardia, F. E., "On Some Unicity Problems in Building System Identification from Strong Motion Records," *Proceedings of the Fifth European Conference on Earthquake Engineering*, 1975.
8. Udwardia, F. E., "Controllability, Observability and Identification of Classical Linear Dynamic Systems," *Solid Mechanics Archives*, Vol. 6, Issue 2, Apr., 1981, pp. 193-211.
9. Udwardia, F. E., Sharma, D. K., and Shah, P. C., "Uniqueness of Damping and Stiffness Distributions in Identification of Soil and Structural Systems," *Journal of Applied Mechanics*, Vol. 45, Mar., 1978, pp. 181-187.